SPIE Proc. Vol. 5531,pp-450-461(2004); "Interferometry XII:Techniques and Analysis."

Propagating Fourier frequencies vs. carrier frequency of a pulse through spectrometers and other media

Chandrasekhar Roychoudhuri, chandra@phys.uconn.edu
Photonics Lab., Physics Department, University of Connecticut, Storrs, CT 06269.

ABSTRACT

In reality, the duration of all light sources (oscillators) is finite. So, effectively, light is always pulsed, whether it is of nano second or of giga second durations. This paper develops a conceptually congruent model of propagating the carrier frequency of a generic pulse directly in the time domain through traditional instruments and media. The modeling approach covers all spectrometers like multi-beam Fabry-Perots and gratings, and two-beam Fourier transform spectrometers. The established approach uses a non-causal Fourier integral to generate Fourier decomposed frequencies of the pulse, which exist in all time, and find their steady state delays through instruments and media. This frequency domain approach gives correct results when appropriately used, but encounters contradictions under some situations that are discussed. In contrast, the time-domain analysis, while mathematically less elegant, always makes correct predictions, besides giving us a deeper and better understanding of the physical processes of temporal evolution of the pulse through various instruments.

Keywords: Temporal interference, pulse spectrometry.

1. INTRODUCTION

Formulation of interference and diffraction patterns with CW, monochromatic light is very simple and well presented in elementary and advanced books [1, 2]. When the incident light is pulsed, the CW formulation is leveraged by propagating the Fourier component frequencies, given by the time-frequency Fourier transform of the incident pulse, centered around the carrier frequency. The approach does give the correct observed result in the cases of optical instruments, specifically, the time integrated, total fringe energy distribution. This approach implies that the amplitudes of different frequencies, when superposed, re-constitute the space and time finite optical pulse; as if, light interferes with light to modify each others energy distribution and the E-vector frequency, even in the linear regime. But, then we face a contradiction with the principle behind the success of the Fourier transform spectroscopy (FTS), namely, light of different frequencies do not influence each other. This non-interference is also evident in our daily lives. If light beams crossing each other were to modify each other, the terrestrial and the cosmic views would have become incessantly glittering space and time speckles. We would have lost the capability of studying and recognizing any distant objects!

The Fourier theorem is based on the linear superposition of sinusoidal functions and Maxwell's wave equation accepts such linear superposition. This could logically lead one to identify the principle of superposition with the Fourier theorem, even though they are not. This point can be appreciated by identifying the steps that makes FTS successful [3]. (i) The two-beam interference fringes are recorded through a quadratic energy exchange process as cosine^2. (ii) This is then "linearized" into a Fourier transformable relation by using simple trigonometric identity and rejecting the "DC component" produced in the process. And, all along one assumes that the amplitudes due to different carrier frequencies have remained independent of each other, implying no superposition effect took place. This calls for explanation as to what interference is. Potential dipoles in material detectors, constrained by their quantum properties, respond (oscillate) to the locally present, superposed electromagnetic fields. (i) The resultant of the field amplitudes determines the strength of the dipole undulation. (ii) Then the short-time average of the square of the resultant amplitude determines only the *probability* (not certainty) of energy transfer through this joint undulation. (iii) The ensemble average of such records allows us to interpret the fringes as interference effects. In the linear space, light does not interfere with light; the interference phenomenon, or the Principle of Superposition, always manifests through the quantum mechanical response of the material dipoles. This is why atomic detectors with sharp energy levels cannot respond to the presence of multiple

frequencies, while the appropriately chosen solid state detectors with broad energy bands can respond, and does show beat signals, meaning multi frequency superposition effects [4]. Such a hard causality (reality) based interpretation is consistent with both the classical physics and the basic prescriptions of quantum mechanics and has also been promoted by Einstein through his famous paper, known as "EPR paper". However, most quantum interpretations disagree with this position. These issues are discussed in a fairly balanced way by Zajonc [5]. Interference, by definition of the word, is the superposition of multiple entities of similar type, and a different entity must be capable of *simultaneously operating, or interacting* on all these superposed entities (causality and physical locality) to register their collective presence. Cause and effect require simultaneous physical presence of all the parties in both space and time in the same physical locality, dictated by the physical size of the detector. This does raise the question as to how one defines (i) a single photon, and (ii) single photon interference [6]. Since, essentially all engineering interference and spectroscopic measurements are carried out with plenty of light, the semi-classical approach (Maxwell's wave and quantum mechanical detector) have successfully explained all interference phenomena by using spreading wave packets and without the need of indivisible photons, defined as modes of a cavity, resembling Fourier components [6].

Accordingly, we devote this paper to develop a generic mathematical formulation for the propagation of the carrier frequency of a wave packet directly in the time-domain (laboratory frame), rather than in the traditional mathematical, Fourier frequency domain. We will demonstrate that the mathematical Fourier theorem is an elegant and a powerful tool and gives correct results when used properly. However, it is not a principle of physics, and, accordingly, care must be taken in its applications and the consequent interpretation of the results. We have developed a coherent methodology to represent all interferometers and diffraction gratings as a Lummer-Gehrcke interferometer [7] through a simple geometrical analogy. We demonstrate that our time domain approach elegantly recovers (i) the traditional CW response, (ii) the time integrated fringe broadening as the traditional convolution of the Fourier intensity spectrum with the CW intensity instrumental response through the use of the Parseval's theorem of energy conservation (time eliminated!). However, it is also capable of computing the time evolving width of the fringe intensity that cannot conform to any Fourier intensity spectrum, which is, by its definition, independent of time.

Section 2 develops the concept of how the ancient Lummer-Gehrcke interferometer can represent all the multiple beam spectrometers (Fabry-Perots and gratings) and all the two-beam interferometers. The section 3 develops the core formulation of this paper by propagating the carrier frequency in the time domain with its wave packet envelope. The section 4 recovers the fringe broadening effect as predicted by the Fourier frequency propagation method, but from the time domain formulation. The section 5 describes how to recover the carrier frequency distribution of any pulsed light from interferograms, represented by time domain formulation, produced either by multiple beam (Fabry-Perots, and gratings), or by two beam (Michelson's FTS) spectrometers. The section 6 highlights the contradictions built into the non-causal Fourier transform integral by propagating an infinite train of periodic pulses by using the Fourier frequencies of the pulse train. In the final section 7, we discuss and summarize the fundamental distinctions between the two approaches of propagating the actual carrier and the mathematical Fourier frequencies.

2. A LUMMER-GEHRCKE GENERICALLY REPRESENTS ALL OTHER INTERFEROMETERS

An air spaced, tilted, Fabry-Perot interferometer (FP), when illuminated by a narrow pencil of CW light, it transmits a regularly, spatially, spaced and phase delayed train of beams as depicted in Fig.1. The structure resembles a Lummer-Gehrcke interferometer (LG) [2, 7]. A focusing lens will produce multiple-beam, Fabry-Perot, fringes on the focal (spatial Fourier transform plane). Since the N-beams emerge from the LG as independent beams, one can imagine them as if they are coming out of the individual steps of an echelon grating, except with periodically reduced amplitudes. The grating-like equality of the amplitudes in the individual steps can, in principle, be restored by appropriately applying graded reflective coatings on the mirrors. A blocking aperture can now control the effective number of "grating slits" [7]. Then, allowing only two beams to emerge would resemble a Michelson-like two-beam interferometer; the variable path delay can be introduced by changing the separation between the two mirrors.

The Fig.2, a, b, & c represent the schematic diagrams of the traditional Fabry-Perot, the echelette grating and the Michelson. If the total step-delay between two consecutive beams is τ, then a single incident pulse will produce a train of pulses with the periodic delay τ, as depicted in this figure. When the input pulse is wider than the step delay, there will

be real physical superposition, albeit partial, between the neighboring pulses in the output train. This is the case of interest to us and is depicted in the Fig.3. For graphical convenience, the echelette grating is presented in transmission, but the formulation assumes its operation in reflection to avoid the complexity of taking care of the material dispersion (frequency dependent velocity of light).

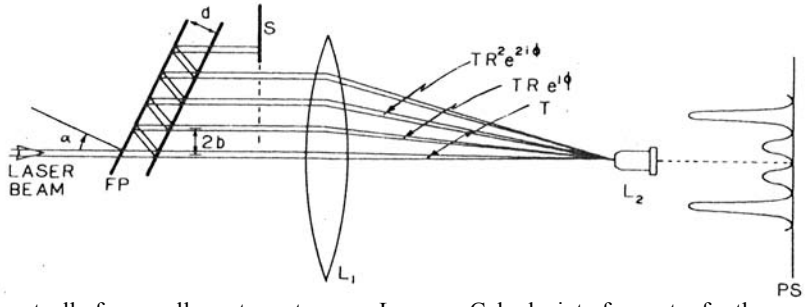

Figure 1. This sketch conceptually frames all spectrometers as a Lummer-Gehrcke interferometer for the convenience of mathematical modeling. A narrow, collimated beam, incident on a tilted Fabry-Perot (FP), generates a train of parallel beams. These beams produce spatial FP fringes in the focal plane of a lens. The multiple beams can also be imagined to be emerging out of an N-slit echelette grating. If one imagines to reduce the number of emerging beams to two with the help of a screen, then one can effectively simulate a two-beam interferometer; changing the plate separation will allow the recording of fringe visibility, as id done by a Michelson's Fourier transform spectrometer [7].

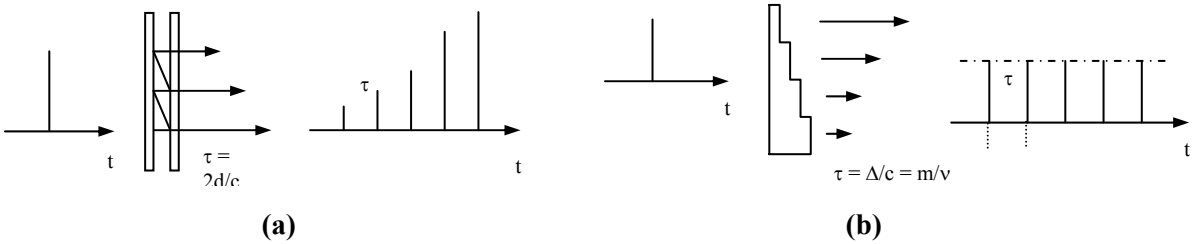

Figure 2. Schematic diagrams for a traditional Fabry-Perot interferometer (a), an echelette grating (b). They show how the replicated and delayed, output pulses would appear due to a single incident ultra short pulse [13].

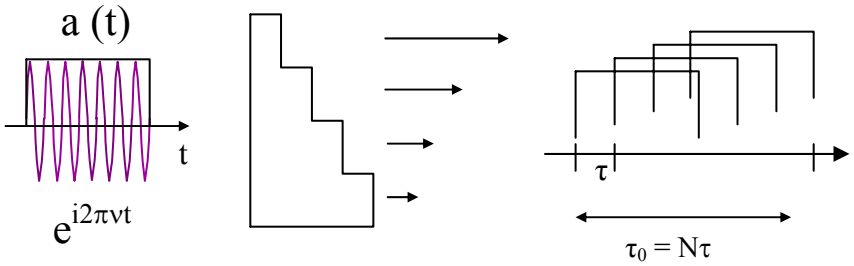

Figure 3. This schematic diagram depicts the partial superposition of a train of finite pulses with a periodic step delay of τ produced by an echelette grating. The carrier frequency, ν, of the E-vector and the time-finite duration of the input amplitude, a(t), is depicted on the left. Notice that all spectrometers have a characteristic time constant for its fringe evolution, or pulse stretching, given by $\tau_0 = N\tau$ [13].

3. PROPAGATING THE CARRIER FREQUENCY OF A TIME-DOMAIN PULSE.

3.1. Time-domain analysis for a generic short pulse.

We now designate an input wave packet of amplitude envelope, a(t), carrier frequency, ν, which is oscillating as cos(2πνt), by the traditional complex representation [2]. Since in interferometry, only the relative phase delay is important, we are ignoring any arbitrary phase factor that the field may have.

$$i_{in} = a(t)\cdot e^{i2\pi\nu t} \tag{1}$$

The advantage of complex representation is that the photo detection process is probabilistically proportional to the short-time average of the square of the real electric field. This short-time average process is built into the process when one takes the product of the complex conjugate with itself. We now represent the train of delayed output pulses as a delayed superposition of the complex amplitudes:

$$i_{out}(t,\nu) = h(t)\otimes a(t)\cdot e^{i2\pi\nu t} = \sum_{n=0}^{N-1}\left[TR^n, or\,\frac{1}{N}\right]\cdot a(t-n\tau)\cdot e^{i2\pi\nu(t-n\tau)} \tag{2}$$

Where,

$$h(t) = \sum_{n=0}^{N-1}\left[TR^n, or\,\frac{1}{N}\right]\cdot \delta(t-n\tau) \tag{2a}$$

For a grating, N is the number of slits and for an FP, N is effectively equal to its theoretical finesse:

$$N = \pi\sqrt{R}/(1-R) \tag{3}$$

For an ideal grating, T = R = 1 and the total amplitude factor for each slit will be divided by N, which is the total number of grating slits. Further, to recover a Michelson interferometer, one only needs to use N = 2. The finite value for N also indicates that all spectrometers have a finite time constant τ_0 to establish its fringe pattern [8]:

$$\tau_0 = N\tau \tag{4}$$

This is the total path delay between the first and the N-th transmitted wave front. This choice for a grating is obvious; there are only N-delayed and replicated pulses from N slits. For an FP, the choice is justified by Born & Wolf's definition of the resolving power of spectrometers as the number of wavelengths in the path difference between the first and the last "effective" interfering wave fronts [2, p-406]. One can write more explicitly [2, p-335]:

$$\mathcal{R} = \nu/\delta\nu = 0.97mN \sim mN = dN/\lambda = \nu\,(N\tau) = \nu\tau_0 \tag{5}$$

Where, ν is the carrier frequency of the signal; d is the grating step delay, or the FP transit delay; and λ is the wavelength of the signal. The relative reduction in intensity, b, of the n-th transmitted beam compared to the first one can be given by:

$$b = I_n/I_1 = T^2R^{2n}/T^2 \text{ ; or, } \ln b = 2n\ln R \tag{6}$$

For a range of moderate to high finesse FP with R = 0.900 to 0.999, the intensity of the N-th beam will be reduced approximately by the same factor of $b = 1.87\times10^{-3}$. So, one can safely terminate the infinite FP series by a finite sum of N-terms. This also strengthens the simple definition of the FP time constant to be $\tau_0 = N\tau$ [Eq.4]. Notice that we do not call τ_0 as the photon life time for an FP, as is popular in the field of cavity ring down spectrometry (CRDS) for measuring absorptance of dilute gas [9].

The time evolving intensity due to pulsed input, I'_{pls}, which will be detected by a fast photo detector, is the square modulus of the complex amplitude of Eq.2:

$$I'_{\text{pls}}(t,\nu,\tau) = \left|i_{out}(t)\right|^2$$

$$= \sum_{n=m=0}^{N-1} T^2R^{2n}a^2(t-n\tau) + 2\sum_{n>m} T^2R^{n+m}a(t-n\tau)a(t-m\tau)\cdot\cos[2\pi(n-m)\nu\tau], \text{ for an FP.} \tag{7}$$

$$= \sum_{n=m=0}^{N-1} \frac{1}{N^2}\cdot a^2(t-n\tau) + 2\sum_{n\neq m} \frac{1}{N^2}\cdot a(t-n\tau)a(t-m\tau)\cdot\cos[2\pi(n-m)\nu_c\tau], \text{ for a grating.} \tag{7a}$$

The center of the fringe for any particular order, m = ντ, is an invariant location on the fringe plane and is deter mined solely by the carrier frequency, ν, even though the width is varying with time. This temporal evolution is due to the change in the number of beams that are simultaneously (physically) present on the detector at any moment, and we know that the fringe width depends upon the number of beams interfering together at any moment. This also underscores our epistemological position that the interference phenomenon is a causal one. The total, time integrated, fringe energy distribution recorded by a photographic plate is given by:

$$I''_{pls}(\nu,\tau)=\sum_{n=0}^{N-1}T^2R^{2n}\int_{-\tau_0/2}^{+\tau_0/2}a^2(t-n\tau)dt+2\sum_{n\neq m}^{N-1}T^2R^{n+m}\cos[(n-m)\nu\tau]\int_{-\tau_0/2}^{+\tau_0/2}a(t-n\tau)a(t-m\tau)dt$$

for an FP. (8)

$$=\frac{1}{N^2}\sum_{n=0}^{N-1}\int_{-\tau_0/2}^{+\tau_0/2}a^2(t-n\tau)dt+\frac{2}{N^2}\sum_{n\neq m}^{N-1}(N-|n-m|)\cos[(n-m)\nu\tau]\int_{-\tau_0/2}^{+\tau_0/2}a(t-n\tau)a(t-m\tau)dt$$

for a grating. (8a)

Where, τ_0 indicates the total length of the replicated pulse train. The relation is simplified by dividing the Eq.8 throughout by the constant, the total, time integrated energy of the pulse:

$$I_{pls}(\nu,\tau)=\sum_{n=0}^{N-1}T^2R^{2n}+2\sum_{n\neq m}^{N-1}T^2R^{n+m}\gamma(|n-m|\tau)\cos[2\pi(n-m)\nu\tau]\text{, for an FP.} \quad (9)$$

$$=\frac{1}{N}+\frac{2}{N^2}\sum_{p=1}^{N-1}(N-p)\gamma(p\tau)\cos[2\pi p\nu\tau]\text{, for a grating.} \quad (9a)$$

Where, $\gamma_{nm}(\tau)$ is the normalized autocorrelation of the amplitude, a(t) with different periodic delays:

$$\gamma(p\tau)\equiv\gamma_{nm}(\tau)\equiv\gamma(|n-m|\tau)=\frac{\int a(t-n\tau)a(t-m\tau)\,dt}{\int a^2(t)\,dt} \quad (10)$$

For both an FP and a grating, the "spectral" fringe broadening, given by Eq. 9 & 9a, can be interpreted as the periodic superposition of cosine fringes due to the same carrier frequency but of different periodicity on a "DC bias". Even though the fringe is broadened, the energy corresponds to the same carrier frequency, ν, emitted by the source. The equation looks complex, but, it makes intuitively obvious the reason behind fringe broadening. It is due to (i) the unequal amplitudes of the beams, R^n, produced by to multiple reflections (same as in CW case), (ii) the partial superposition of a finite number of pulses at any particular detection interval, and (iii) the time evolving amplitudes due to pulse envelope characterized by γ (see

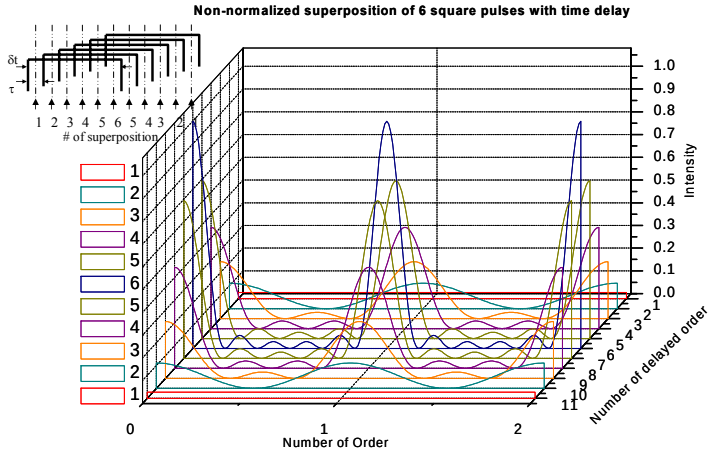

Figure 4. Time evolving fringe width due to a single rectangular pulse transmitted through a Fabry-Perot interferometer. The number of superposed pulses increases with time, producing narrower fringes. The process then reverses with fringe broadening again. When a photographic plate integrates all these time varying fringes, we get a broader interference fringe compared to a CW illumination with the same carrier frequency [13].

Fig.3). We call this fringe broadening *pulse-impulse response*. Just as we accept for CW light that the *CW-impulse-response,* $\delta\nu_{cw,}$ does not represent any new optical frequencies, same is also true for $\delta\nu_{pulse}$, representing the *pulse-*

impulse response. That the "spectral" fringe broadening due to a pulse is an artifact of the time varying amplitudes, can be further appreciated by plotting the *time-resolved* fringes from the Eq.7, as shown in Fig.4. The fringe width evolves from initial infinity (no fringes) to a reasonably narrow one (never narrower than the CW case), and then again broadens out to infinity. The total time integrated energy distribution, after the entire pulse train has passed though the detector, gives us the measured energy distribution and the final fringe width, given by the Eq.9. Note that the time varying fringe width of Fig.4 cannot be interpreted as real, physical, time varying optical frequencies by any known hypothesis or principle of Physics. The functional shape and the width of the Fourier transformed frequency function, $\tilde{a}(f-\nu)$, is a well defined and a *time-invariant function*, and hence, it cannot be identified with the time varying fringes [10]. A linear device like an FP, or a grating, can neither produce, nor respond to the mathematical Fourier frequencies. The time-frequency FT represents a non-causal integral, requiring some memory to read the entire envelope that moves with a finite velocity, and hence takes a finite time to travel through the FP.

3.2. CW case as an infinitely long pulse.

CW case can be considered as a special case when the incident pulse is infinitely long. Under this circumstance, all the autocorrelation factors, $\gamma(|m-n|\tau)$, are unity, and we obtain the CW instrumental response for a monochromatic radiation of carrier frequency, ν, as a summation of a large number of two-beam interference with all possible delays, (m-n)τ, riding over a DC bias:

$$I_{cw}(\nu,\tau)=\sum_{n=0}^{N-1}T^2R^{2n}+2\sum_{n\neq m}^{N-1}T^2R^{n+m}\cos[2\pi(n-m)\nu\tau], \quad \text{for an FP.} \tag{11}$$

$$=\frac{1}{N}+\frac{2}{N^2}\sum_{p=1}^{N-1}(N-p)\cos[2\pi p\nu\tau], \text{ for a grating.} \tag{11a}$$

We have thus established the conceptual continuity for the fringe width between those produced by a short pulse and a very long pulse, because $\gamma(p\tau)\to 1$ as the pulse width, $\delta t\to\tau_0=N\tau$, underscoring the significance of τ_0, defined by us as the spectrometer time constant [8]:

$$\underset{\delta t\to\tau_0=N\tau}{Lt.}\left[I_{pls}(\nu,\tau)\right]=I_{cw}(\nu,\tau) \tag{11b}$$

Computed curves to demonstrate this convergence has been presented elsewhere [13] using this formulation and FDTD method. Thus, propagating the carrier frequency gives a remarkable similarity between the location and the origin of the width of the fringes due to a very short and an infinitely long pulse; the location of the center of the fingers are always determined by the carrier frequency through the relation for the fringe order, m = ντ. Of course, the fringe energy is spread over more area (broader fringe) for a short pulse due to the autocorrelation terms than for an infinitely long pulse. The Eqns. 11 & 11a represent the *CW instrumental response* function and the Eqns. 9 & 9a represent the *pulse instrumental response*. The excess width of Eqns. 9 & 9a do not represent the generation of any new optical frequencies. We will now establish the correctness of the Eqns. 11 & 11a, since they are not used traditionally in any text books, to our knowledge.

3.3. CW case through delta impulse response and Fourier transformation.

Let us consider the case of a single, infinitely narrow, optical impulse of amplitude, δ(t). This will be useful for some mathematical manipulations. This single impulse, after passing through the FP or the grating, generates a train of transmitted pulses, given by:

$$h(t)=\sum_{n=0}^{N-1}\left[TR^n, or\ \frac{1}{N}\right].\delta(t-n\tau) \tag{12}$$

The Fourier transform of this transmitted amplitude response, assuming the transforming Fourier kernel to be exp [-i2πft], is given by:

$$\tilde{h}(f)=\sum_{n=0}^{N-1}\left[TR^n, or\ \frac{1}{N}\right]e^{i2\pi nf\tau}=\left[\frac{T}{1-R\,\mathrm{e}^{i2\pi f\tau}}\right]_{FP}, or\ \frac{1}{N}\left[\frac{1-\mathrm{e}^{i2\pi Nf\tau}}{1-\mathrm{e}^{i2\pi f\tau}}\right]_{grating} \tag{13}$$

For an FP, the factor $(1-R^N\,\mathrm{e}^{i2\pi Nf\tau})$ in the numerator has been reduced to unity assuming R^N reduces to zero for high finesse devices (see Eq.6). This allows one to reconcile our finite sum approach with the expression for the traditional

infinite sum found in all text books [2]. Eq.13 represents expressions that are identical to CW, monochromatic light [2], except that the frequency, f, has been generated by the Fourier transform kernel, rather than by any electromagnetic oscillator. That is because we started with an arbitrarily narrow, time domain, impulse function. However, one can also follow the standard text book approach [2] of starting with a steady state CW, monochromatic radiation with a carrier frequency, ν, and derive the same expressions as in Eq.13, replacing f by ν. However, the mathematical utility of Eqns.13 and 14 (below) will be apparent in the next section. The CW fringe intensity can now be derived two ways. In the first approach, one can take the square modulus of the expressions on extreme RHS of the Eq.13 and again derive the traditional expressions for the intensities of the CW fringes:

$$\tilde{H}(f) \equiv \left|\tilde{h}(f)\right|^2 \equiv I_{out,CW}(f) = \left[\frac{T^2}{(1-R)^2 + 4R\sin^2 \pi f \tau}\right]_{FP}, or \left[\frac{1}{N^2}\frac{\sin^2 \pi N f \tau}{\sin^2 \pi f \tau}\right]_{grating} \tag{14}$$

The other alternative is to literally take the square modulus of the sum directly as $\Sigma^*\Sigma$. For an FP, it is:

$$\begin{aligned}\tilde{H}(f) \equiv I_{cw}(f) &= \left(\sum_{m=0}^{N-1} TR^m e^{-i2\pi m f \tau}\right)\left(\sum_{n=0}^{N-1} TR^n e^{i2\pi n f \tau}\right) \\ &= \sum_{n=0}^{N-1} T^2 R^{2n} + 2\sum_{n\neq m}^{N-1} T^2 R^{n+m}\cos[2\pi(n-m) f \tau], \quad \text{for an FP.}\end{aligned} \tag{15}$$

For a grating, we have:

$$\begin{aligned}\tilde{H}(f) \equiv I_{cw}(f) &= \left(\frac{1}{N}\sum_{m=0}^{N-1} e^{-i2\pi m f \tau}\right)\left(\frac{1}{N}\sum_{n=0}^{N-1} e^{i2\pi n f \tau}\right) \\ &= \frac{1}{N} + \frac{2}{N^2}\sum_{p=1}^{N-1}(N-p)\cos[2\pi p f \tau], \qquad \text{for a grating.}\end{aligned} \tag{15a}$$

$\tilde{H}$ of Eqns.15 and I_{cw} of Eqns.11, both represent the same CW fringe intensity distribution, or *CW impulse response* when one interchanges f and ν. The Eqns. in 15 are identical in structure to those in Eqns.11 that were derived from Eqns.9 for generalized *pulse impulse response* by taking the autocorrelation terms equal to unity for infinitely long pulse. This establishes our claim that propagating the carrier frequency of a generic pulse is intuitively more appealing as it reveals the source of fringe broadening as instrumental artifact, coupled with the pulse width, rather than the presence of any new optical frequencies. Confusion may sometimes arise due to the identical sinusoidal structures of the solution to Maxwell's wave equation and the kernel of the mathematical transform theorem developed by Fourier.

4. PROPAGATING THE FOURUER FREQUENCIES OF A PULSE

Let us now derive the time integrated fringe broadening from the frequency domain analysis. The Fourier transform of the amplitude envelope, a(t), traced out in time by the E-vector-amplitude of the carrier frequency, ν, is:

$$FT[a(t)e^{i2\pi\nu t}] = \tilde{a}(\nu - f) \tag{16}$$

The Fourier kernel, as before, is $\exp[-i2\pi ft]$. Please, note that the time varying excursion of the E-vector-amplitude, by Maxwell's theory, is a real, physical parameter of the signal. But, the envelope a(t) is only a mathematically convenient and approximate representation of this excursion. From Eq.2, the Fourier transform of the transmitted, out put pulse train, $i_{out}(t)$, is given by:

$$\tilde{i}_{out}(f) = \tilde{h}(f)\cdot\tilde{a}(\nu - f) \tag{17}$$

The corresponding intensity in the Fourier space can be represented as:

$$\left|\tilde{i}_{out}(f)\right|^2 = \tilde{H}(f)\cdot\tilde{A}(\nu - f) \tag{18}$$

Let us now apply the Parseval's theorem of energy conservation on Eq.18 and the transmitted pulse train whose amplitude is given in Eq.2:

$$\int_{-\infty}^{\infty} |i_{out}(t)|^2 dt = \int_{-\infty}^{\infty} |\tilde{i}_{out}(f)|^2 df \tag{19}$$

$$= \int_{-\infty}^{\infty} \tilde{H}(f) \cdot \tilde{A}(\nu - f) df = \tilde{H}(\nu) \otimes \tilde{A}(\nu) \tag{19a}$$

Or, $$\int_{-\infty}^{\infty} |i_{out}(t)|^2 dt = I_{cw}(\nu) \otimes \tilde{A}(\nu) \tag{20}$$

The Eq.19a is re-written by identifying the mathematical similarity between $\tilde{H}$ and I_{cw}. The Eq.20 is a very important relation, as it establishes the *quantitative equivalency* between the spectrometer fringes (FP's and gratings) due to a pulsed light calculated in two independent ways, by time domain and Fourier frequency domain analyses. The RHS of Eq.20 represents the traditional interpretation of spectrometer fringes produced by a pulse. It tells us that the "spectral" fringe broadening in a FP due to a pulse with a single carrier frequency can be obtained mathematically by simply convolving the Fourier spectral intensity of the incident pulse with the *CW-impulse-response*. One should note that the mathematical equivalency of the two sides in Eq. 20 is achieved after the time has been eliminated in both the approaches through integration by employing Parseval's theorem on energy conservation. This step eliminates the non-causal aspect of the time-frequency Fourier integral. The realization that this fringe broadening is simply due to spreading of energy of the same carrier frequency, and not due to the presence of any new optical frequencies, opens up new way of implementing spectrometric super resolution [13] beyond the generally claimed fundamental limit, $\delta f \delta t \geq 1$.

5. SPECTROMETRY AS RECOVERY OF THE DISTRIBUTION OF THE SOURCE CARRIER FREQUENCIES

5.1. Multiple beam spectrometers (Fabry-Perots and gratings).

In general, all optical signals to be spectrometrically analyzed are pulsed, whether the duration is nano seconds or Giga seconds. Even a CW laser and/or the detector have to be turned on and off. Thus, we prefer our generic approach of propagating the carrier frequencies with their pulse amplitude envelopes, as developed in section 3. The *pulse impulse response*, I_{pls} (ν, τ), given by Eqns.9 & 9a is to be utilized to analyze complex source spectrum. We assume that the complex, normalized spectral intensity, $S_{in}(\nu)$, is produced by the identical shaped amplitude envelopes, a(t). We can imagine that S_{in} (ν) has been generated from a CW, multi longitudinal mode laser with an ideal, external amplitude modulator. We know that different optical frequencies do not influence each other on the interferometer beam splitters (or, at the grating teeth). So, the out put fringe pattern, S_{out} (ν), generated by S_{in} (ν) can be given by the convolution of the source spectrum with the *pulse impulse response* of the spectrometer, and not the *cw impulse response*:

$$S_{out}(\nu) = S_{in}(\nu) \otimes I_{pls}(\nu, \tau) \tag{21}$$

$$S_{in}(\nu) = S_{out}(\nu) \otimes^{-1} I_{pls}(\nu, \tau) \tag{22}$$

The recovery of the source spectrum, S_{in} (ν), the distribution of the actual carrier frequencies, will require deconvolution of the *pulse impulse response*, Ipls (ν, τ), from the recorded interferogram, S_{out} (ν), as in Eq.22. A practical example of S_{in} (ν) could be the Doppler broadened atomic pulses from a gas discharge lamp, provided we impose the assumption that excited atoms emit classical light pulses, or wave packets with unique carrier frequencies. Now, a careful observation of Eq.22 reveals a conflict with the traditional approach in spectrometry because it is customary to use I_{cw} (ν, τ) of Eq.11, or $\tilde{H}(\nu)$ of Eq.15, instead of Ipls (ν, τ) for deconvolution. Since I_{pls} (ν, τ) is broader than I_{cw} (ν, τ), our time domain analysis predicts a narrower intrinsic line width for gas discharge spectrum than the established approach. Further discussion on this point will be published else where.

5.2. Two beam, or Michelson's Fourier transform spectrometer.

Traditional Fourier transform spectroscopy is carried out by Michelson's two-beam interferometer. The generic pulse impulse response for a Michelson is derived from Eq.9a for a grating by inserting N = 2:

$$I_{pls,2}(\nu) = \frac{1}{2}\left[1 + \gamma(\tau)\cos(2\pi\nu\tau)\right] \tag{23}$$

As in the last section, let us consider that we have recorded a Fourier transform interferogram, $S_{out,2}(\nu)$ of a gas discharge lamp, emitting identical pulses, a (t), with intensity distribution of the carrier frequencies, S_{in} (ν):

$$S_{out,2}(\nu) = S_{in}(\nu) \otimes I_{pls,2}(\nu,\tau) \tag{24}$$

$$S_{in}(\nu) = S_{out,2}(\nu) \otimes^{-1} I_{pls,2}(\nu,\tau) \tag{25}$$

Traditionally, the "DC component" of the interferogram, $S_{out,2}(\nu)$, would be removed to recover the oscillatory component of the interferogram [3], which would then be Fourier transformed (notice the cosine term in Eq.23) to recover the apparent source "spectrum". That is very different from what we predict through our time domain analysis and the recovery process for S_{in} (ν) given by Eq.25; it is a deconvolution

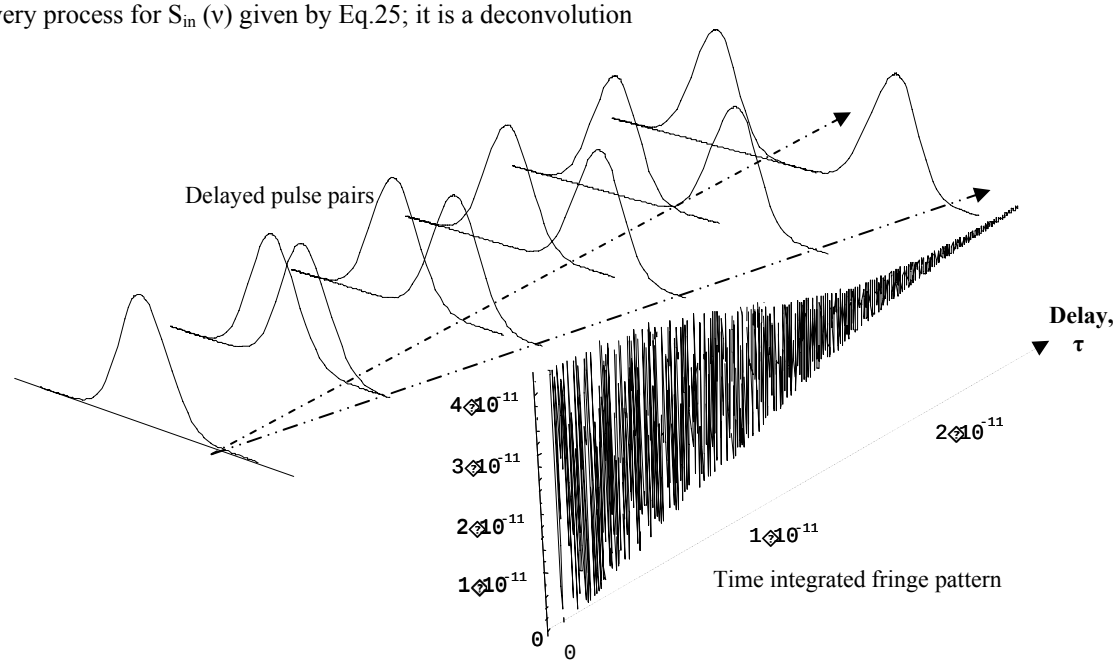

Figure 5. Variation of long-time integrated, fringe visibility in a simple Michelson interferometer as the delay between the mirrors is varied. The pulse, a (t) exp [i2πνt], is considered perfectly reproducible and the time integrated fringe energy is recorded separately for each delay position, τ. The resultant visibility of the fringes, degraded by γ (τ), is due to superposition of unequal amplitudes on the detector.

process that is more complex than the simple Fourier transform. This is specifically because the time domain analysis considers the visibility degradation factor, γ (τ), as an artifact of interference between two unequal amplitudes due to two translated pulses that has nothing to do with the distribution of actual frequencies of the electromagnetic field.

Let us look at the origin of γ (τ) from the pulse, a (t) exp [i2πνt], with a single carrier frequency, superposed with a displacement τ by the two-beam interferometer. If the interferogram (Eq.23) were generated by a pulse from a CW, single frequency laser with an external amplitude modulator, it could recover the carrier frequency, ν, simply by counting the fringes, cos(2πντ), with τ, albeit the difficulty due to reduced visibility, γ(τ):

$$V = \frac{I_{\max} - I_{\min}}{I_{\max} + I_{\min}} = \gamma(\tau) \tag{26}$$

This degradation of the fringe visibility is due to superposition of varying amplitudes at varying delays, τ, as illustrated in Fig.5. By Wiener-Khintchine theorem [2], one can express γ (τ) as the Fourier transform of the square modulus of the Fourier transform, $\tilde{A}(f)$ of the original pulse amplitude, a (t):

$$\gamma(\tau) \approx \int \tilde{A}(f) e^{-i2\pi f\tau} df \tag{27}$$

Notice several interesting features of the Wiener-Khintchine theorem. The traditional approach of replacing $\gamma(\tau)$ by $\tilde{A}(f)$ does not add any new useful knowledge about the original source frequency at all [11]. The origin of the frequency, f, is from the Fourier kernel, and it has nothing to do with the source (electric vector) frequency, ν. Second, the Fourier frequencies, f, were generated by an integral whose Fourier transform pair consists of time and frequency. Third, this Fourier mathematical frequency, f, is integrated out in the Eq.27, to leave behind the experimental delay parameter, τ, because here the pair of variables for the Fourier transformation is the frequency and the delay time, f and τ, not the frequency and the running time, ν and t that generated f to reconstruct a(t). Fourth, the integration is carried over the intensities of all the Fourier frequencies, not the amplitudes. The amplitudes of different optical frequencies do not influence each other on beam splitters. This is the fundamental assumption by Michelson behind the success of his experimental Fourier spectrometry. Thus, by virtue of the relation of Eq.20 (Parseval's theorem, Eq.19), we have mathematical self consistency between the measured, time integrated, fringe energy distribution derived by two different approaches. However, we must acknowledge the profound contradiction in the principle of Physics. Optical beams of different source (carrier) frequencies, when superposed, do not interfere with (or, modify) each other. Whereas, synthesizing back an optical pulse through its Fourier decomposed monochromatic frequencies through superposition, demands interference between different optical frequencies.

6. PROPAGATING FOURIER FREQUENCIES THROUGH A FIBER

A direct time domain propagation of a single or a train of pulses, through a spectrometer will always produce a stretching of the out put pulse by approximately $\tau_0 = N\tau$, as depicted in Fig.3, due to delayed superposition of the replicated pulses produced by the spectrometer, even in a dispersion free space. In contrast, propagation of the Fourier frequencies of a pulse through a tilted FP mirrors in free space [see Fig.1; ignore mirror thickness] should not produce any pulse broadening, only delayed superposition. In this section, we highlight the contradictions encountered in propagating mathematical Fourier frequencies through a real dispersive medium. We have computer simulated the propagation of Fourier frequencies for an infinite train of pulses, which is generated by an external, ideal amplitude modulator from a CW, single frequency laser. One can also assume that the infinite train of pulses has been produced by a multi mode laser with ideal mode locking contraptions. The traditional approach [12] to compute the dispersion broadening of a single pulse is to propagate the Fourier transformed frequencies of the pulse through the material medium and then superpose them with the dispersive phase delays suffered by each Fourier frequency. The dispersive phase delays for a continuous distribution of frequencies (infinite number) always produces pulse broadening due to continuously varying relative phase delays. In contrast, if the number of monochromatic frequencies is finite, as in the Fourier transformation of an infinite train of periodical pulses, it is always possible to find a finite length of a dispersive medium that produces "modulo-two-pi" phase delays for each of the frequencies in the set. Then their superposition will regenerate the original pulse train without any dispersive pulse broadening [14]. This is a linear propagation, and hence the effect should not be identified with solitons. The computer simulation is presented in the Fig.6. This "waxing and waning" of the fringe width is mathematically identical to the fringe visibility that would be produced by a Michelson interferometer for the same set of CW, monochromatic frequencies. The resolution of these contradictions will be discussed elsewhere.

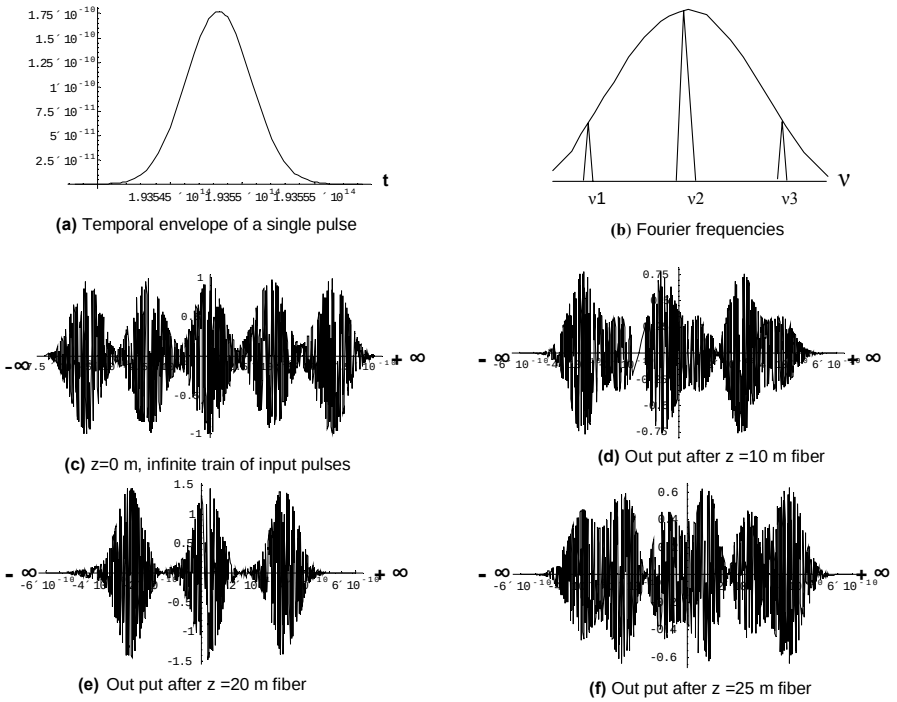

Figure 6. A Gaussian pulse, shown in (a), is periodically repeated infinite times (c), which gives a finite set of Fourier frequencies, shown in (b). Mathematically, the superposition of these frequencies regenerates the infinite train of pulses, shown in (c). When these frequencies are propagated individually through a fiber of finite length with appropriate refractive indices, and then superposed at the out put plane, one re-generates the pulse train, but with "dispersion broadening effect", shown in (d, e, & f) due to differential phase delays experienced in propagating through different lengths of fibers [12]. For a finite set of monochromatic frequencies, one can always find a finite length of a fiber, for which the differential phase delays are modulo-two-pi, which reproduces the original pulse train without any pulse dispersion, as shown in (e) [14].

7. CONCLUSION

The strength of this paper lies on its capability to demonstrate conceptual congruency amongst all the spectrometers, multiple-beam or two-beam, through a common mathematical formulation based on hard causality, which is propagating the actual carrier frequency emitted by a source aided by its temporal wave packet envelope. The process also demonstrates the conceptual continuity between the "spectral" fringes produced by a short wave packet and an arbitrarily long wave packet (pulse). The fringe broadening is an instrumental artifact dictated fundamentally by the real, physical, and simultaneous presence of the number of interfering beams on the detector. Accordingly, we have concluded that the "spectrum" of an electromagnetic signal should be defined as the actual carrier frequency distribution, generated by the quantum mechanical dipole oscillators. Notwithstanding the mathematical correctness of the Wiener-Khintchine theorem, the Fourier transform of the autocorrelation function of the pulse under investigation should not be used as the physical spectrum, because the fringe visibility can be influenced by both the actual carrier frequency distribution and the superposition of unequal amplitudes of a translated pulse. Otherwise we loose the distinctions between the CW light from a multi-frequency, CW laser and the externally modulated amplitude pulses from a single-frequency, CW laser. Both these electromagnetic fields can be designed to give the identical, periodically oscillating, fringe visibility over a wide range of path delays in a Michelson interferometer. It will be unfortunate to consider the "spectrum" to be identical for both the lasers. Our time domain formulation of propagating the actual carrier frequencies can clearly distinguish between the two sources. We believe, it is the non-causality of the time-frequency Fourier transform that introduces the contradictions.

8. ACKNOWLEDGEMENTS

The author would like to acknowledge the support of DongIk Lee for the computer plots of Fig.4 and Fig.5 and Yongyuan Jiang for the plots of Fig.6. Qing Peng also provided some help to prepare this manuscript. Further acknowledgement is due to the Nippon Sheet Glass Company for partial support of this research.

9. REFERENCES

1. Eugene Hecht, *Optics,* Addison-Wesley, 1998.
2. Max Born & Emil Wolf, *Principles of Optics*, Cambridge University Press, 1999.
3. Miles V. Klein, *Optics*, John Wiley & Sons, 1970.
4. DongIk Lee and C. Roychoudhuri, "Measuring properties of superposed light beams carrying different frequencies", Optics Express **11**(8), 944-51, (2003); [http://www.opticsexpress.org/abstract.cfm?URI=OPEX-11-8-944]
5. See discussions on locality and reality in A. G. Zajonc, *The Quantum Challenge*, Jones & Bartlett, 1997.
6. C. Roychoudhuri & R. Roy, Guest Editors, OPN Trends --"The Nature of Light: What is a Photon?", special issue of Optics and Photonics News, October, 2003; [http://www.osa-opn.org/abstract.cfm?URI=OPN-14-10-49]
7. C. Roychoudhuri, "Demonstration Using a Fabry-Perot. I. Multiple-Slit Interference", Am. J. Phys. 43 (12), 1054 (1975)
8. C. Roychoudhuri, "Response of Fabry-Perot interferometers to light pulses of very short duration", J. Opt. Soc. Am.; 65 (12), 1418 (1976).
9. K. K. Lehmann, "The superposition principle and cavity ring-down spectroscopy," J. Chem. Phys., **105**, 10263-10277 (1996).
10. L. Mandel, "Interpretation of instantaneous frequencies," Am. J. Phys. 42, 840-846 (1974).
11. C. Roychoudhuri, "Is Fourier Decomposition Interpretation Applicable to Interference Spectroscopy?", Boletin Inst.Tonantzintla, **2** (2), 101 (1976).
12. Ajoy Ghatak, *Introduction to Fiber Optics*, Cambridge University Press, 1998.
13. C. Roychoudhuri, D. Lee, Y. Jian, S. Kittaka, M. Nara, V. Serikov and M. Oikawa, "Limits of DWDM with gratings and Fabry-Perots and alternate solutions", Invited paper, ITCom Conference; Proc. SPIE Vol.**5246**, pp.333-344, (2003).
14. C. Roychoudhuri and Yongyuan Jiang, "Fourier transforms in classical optics", Conference paper # EMI 10, Education & Training in Optics and Photonics (ETOP), 2003.